A comparative study of Ar and H_2 as carrier gases for the growth of SiC films on Si(100) by electron cyclotron resonance chemical vapor deposition at low temperature

Wen-Horng Lee[a], Jing-Cheng Lin[a], Chiapyng Lee[a,*], Huang-Chung Cheng[b], Tri-Rung Yew[c]

[a]*Department of Chemical Engineering, National Taiwan University of Science and Technology, Taipei 10672, Taiwan, ROC*
[b]*Department of Electronics Engineering, National Chiao-Tung University, Hsinchu 30050, Taiwan, ROC*
[c]*United Microelectronics Corporation, Science-Based Industrial Park, Hsinchu, Taiwan, ROC*

Abstract

Electron cyclotron resonance chemical vapor deposition (ECR-CVD) of SiC films from silane and methane gas mixtures at low temperature has been investigated using two different carrier gases, namely, argon and hydrogen. The results obtained are compared. The chemical composition and crystalline microstructure were investigated by Fourier transform infrared spectroscopy (FTIR) and cross-sectional transmission electron microscopy (XTEM), respectively. The results indicate that the carrier gases have a greater influence on the film composition and microstructure as compared to the growth parameters like pressure, power and flow ratio. The deposition mechanism which controls the film characteristics is also presented. © 2001 Elsevier Science B.V. All rights reserved.

1. Introduction

Silicon carbide (SiC) is an attractive semiconductor material for high-temperature, high-power, and high-frequency device applications because of its superior properties such as high thermal conductivity, high-melting point, high breakdown field, high saturated drift velocity, small dielectric constant, and large band gap, etc. [1–3].

On the other hand, its chemical inertness, transparency over a broad range of wavelength, and hardness can be used as heat-sinking, optical filter anti-reflection hard coatings, X-ray mask, and corrosion-resistant materials. Furthermore, SiC can also be used as a thin buffer layer for the growth of diamond films on silicon [4] and growth of GaN films on α-Al_2O_3 [5].

Conventional ways of depositing SiC films by CVD methods were carried out in a high-temperature environment. A high-temperature CVD process is not suitable for growing SiC films, because it may cause auto-doping, redistribution of dopants in the Si substrate and non-abrupt heterojuctions between SiC and silicon. From the viewpoint of device fabrications, low temperature growth is desired. A relatively new technique, known as electron cyclotron resonance chemical vapor deposition (ECR-CVD) has the ability to deposit β-SiC (3C-SiC) at low temperatures [6,7].

* Corresponding author. Tel.: +886-2-27376623; fax: +886-2-27376644.
  E-mail address: cl@ch.ntust.edu.tw (C. Lee).

Although there have been previously reported investigations on the effects of growth parameters [7−9], the effect of different carrier gases has not been discussed yet. In this paper, the effects of different carrier gases were investigated by varying growth parameters such as total pressure, microwave power, and CH_4/SiH_4 flow ratio. The purpose of this work is to correlate the variation of film chemical composition and crystalline microstructure to the carrier gases. A mechanism which governs the correlation is proposed.

2. Experimental

Silicon carbide (SiC) films were deposited in a commercial Plasma-Quest Model-357 ECR-CVD reactor using $CH_4/SiH_4/H_2$ or $CH_4/SiH_4/Ar$ gas mixtures. The ECR-CVD system configuration has been described elsewhere [8].

The substrates used were (100) oriented, p-type silicon wafers with a resistivity of 5−15 Ω-cm, and were cut into 15×30-mm pieces. The substrates were ex situ cleaned by a modified spin-etching method [10] to provide a hydrogen-terminated silicon surface and prevent surface oxidation during air exposure [11]. The substrate was then loaded into the reactor within a few minutes after cleaning.

The effect of total pressure was investigated by keeping the temperature at 200°C, microwave power at 1200 W and CH_4, SiH_4, and H_2/Ar flow rates at 5, 2.5 and 100 sccm, respectively. Then, the effect of the microwave power was investigated by keeping the temperature at 200°C, total pressure at 20 mtorr, and CH_4, SiH_4, and H_2/Ar flow rates at 5, 2.5 and 100 sccm, respectively. The effect of CH_4/SiH_4 flow ratio was investigated by keeping the temperature at 200°C, microwave at 1200 W, and H_2/Ar flow rates at 100 sccm. The CH_4/SiH_4 flow ratio was varied by changing CH_4 flow rate while keeping SiH_4 flow rate at 5 sccm. The deposition time was 30 min in all cases.

The gas phase species in the plasma were examined by optical emission spectroscopy during the SiC film growth. An optical emission spectrometer (OES, OEA-6850, Rees Instruments Ltd.) was attached to the chamber through one of the ports. Optical emission from the plasma was measured through the side viewing port with the quartz window by multi-channel photodetector system. This system can detect lights with wavelength between 200 and 900 nm. Fourier transform infrared spectroscopy (FTIR) spectra were obtained with a BIO-RAD FTS-40 spectrometer from 400 to 4000 cm^{-1}, with a resolution of 4 cm^{-1} and 16 scan times.

The crystalline structure of the deposited film was examined in a JEOL 2000FX STEM. The samples used for cross-sectional transmission electron microscopy
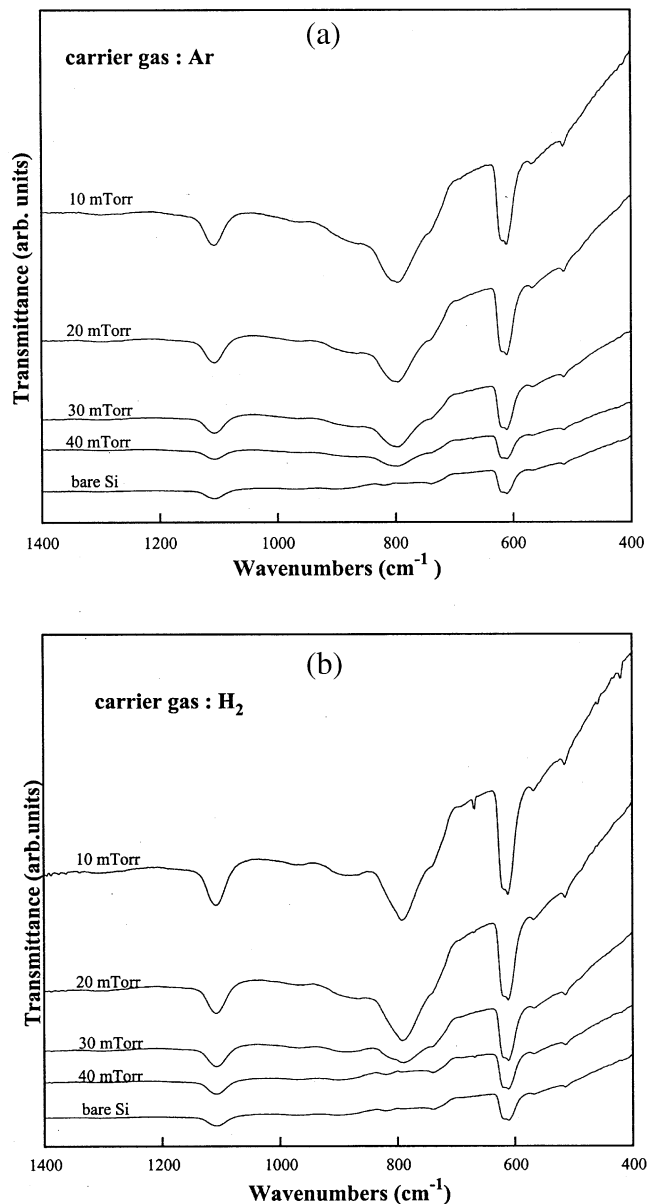

Fig. 1. FTIR transmission spectra of the Si substrate and the films deposited at 200°C, 1200 W, $CH_4/SiH_4 = 2$, various pressures, with (a) Ar as the carrier gas, and (b) H_2 as the carrier gas.

(XTEM) inspection were cut into 2×5-mm size. The XTEM is a destructive analysis technique to observe the deposited film with electron beams perpendicular to the wafer surface normal. As XTEM can be used to observe the deposited film and the film/substrate interface simultaneously, it becomes the most direct and precise way to determine the crystalline phase and lattice constant of the deposited films.

3. Results

Fig. 1a,b shows the FTIR spectra of the bare silicon wafer and films grown at 200°C, 1200 W, $CH_4/SiH_4 =$

2, and various total pressures for Ar and H_2 used as the carrier gas, respectively. From the previous works [12–14], it is known that the Si–C stretching vibration mode of β-SiC occurs at approximately 800 cm^{-1}. The weak peaks at approximately 600 and 1100 cm^{-1} are due to Si and SiO$_2$, respectively. In Fig. 1a (Ar is the carrier gas), all the spectra except bare Si substrate, exhibit the main peak at 800 cm^{-1} of the Si–C bond. However, we can clearly observe in Fig. 1b (H_2 is the carrier gas) that when the total pressure is 40 mtorr, the spectrum only exhibits peaks of Si and SiO$_2$, which are the same as those of the bare Si substrate. When the total pressure is lower than 40 mtorr, the peak appears at 800 cm^{-1} indicates the formation of SiC. The above results indicate that with Ar as a carrier gas, SiC can be grown in a larger pressure range (10–40 mtorr) than with H_2 as a carrier gas (10–30 mtorr).

In order to investigate the difference between Ar and H_2 in gas phase decomposition efficiency, optical emission spectra were recorded. Typical optical emission spectra for $CH_4/SiH_4/Ar$ and $CH_4/SiH_4/H_2$ plasmas at 200°C, 1200 W, and $CH_4/SiH_4 = 2$ are shown in Fig. 2a. The major species observed are H_2^* (220 nm), Si (244, 252, 288 and 390.6 nm), SiH (414 nm), CH (431 nm), H_α (656 nm), H_β (486 nm) and Ar (696.5, 750.4 and 811.5 nm) [15]. The CH (431 nm)/H_α (656 nm) emission intensity ratio as a function of total pressure is shown in Fig. 2b. The CH (431 nm)/H_α (656 nm) emission intensity ratio changes slightly vs. total pressure for Ar discharge, whereas for the H_2 plasma the ratio changes significantly.

Figs. 3 and 4 show the dark-field and bright-field cross-sectional TEM (XTEM) micrographs with electron diffraction patterns of the films grown under the same conditions as those of Fig. 1 when Ar and H_2 were used as the carrier gas, respectively. The XTEM micrograph of polycrystalline silicon grains embedded in amorphous SiC was shown in Fig. 3a (Ar is the carrier gas), which was deposited at a total pressure of 40 mtorr. Fig. 3b indicates that at a total pressure of 30 mtorr, the deposited films on Si are of microcrystalline SiC (μc-SiC) determined by the ring spacing of the electron diffraction pattern. The grains shown in the dark-field image (Fig. 3b) were of μc-SiC, since they were taken from the SiC⟨111⟩ ring of the diffraction pattern. When the total pressure was decreased to 20 mtorr and lower, the polycrystalline β-SiC could be deposited as shown in Fig. 3c. Using the spot diffraction pattern of ⟨110⟩ Si zone in Fig. 3c as a reference, the film is identified to be zinc-blend structure with a lattice constant of 0.436 ± 0.005 nm, which is identical to that of bulk β-SiC [16]. The grains shown in the dark-field image are of SiC since they were taken from the SiC⟨111⟩ ring of the diffraction pattern.

Microstructures of the films grown at different total pressures using H_2 as the carrier gas were also investi-gated and the results are shown in Fig. 4. When the total pressure is 40 mtorr, Fig. 4a indicates that only polycrystalline Si is deposited. At a total pressure of 30 mtorr, the film which is composed of amorphous SiC and embedded polycrystalline Si grains (a-SiC + poly-Si) is deposited as shown in Fig. 4b. However, when the total pressure is decreased to 20 mtorr and lower, polycrystalline β-SiC films are deposited as shown in Fig. 4c. Therefore, compared with Ar (Fig. 3) a lower total pressure (20 mtorr) is required to deposit poly-crystalline SiC when H_2 is used as the carrier gas. The XTEM results are consistent with those obtained by FTIR (Fig. 1).

Experiments with various microwave powers were conducted at a fixed SiH_4 flow rate of 2.5 sccm, 20 mtorr total pressure, and 200°C. The CH_4/SiH_4 flow ratio was kept constant at 2. Compared with the FTIR spectrum obtained from the substrate (bare Si), other spectra in Fig. 5a show that no Si–C bond is formed until microwave power is increased to 500 W. The full width at half-maximum of the peak at 800 cm^{-1} becomes narrower when the microwave power is increased further above 500 W, which indicates that film crystallinity is improved with increasing microwave power. The results shown in Fig. 5b are similar to the results shown in Fig. 5a, when H_2 is used as the carrier gas.

When the total pressure and microwave power were fixed at 20 mtorr and 1200 W, respectively, variation in the CH_4/SiH_4 flow ratio changed the composition of the film significantly as determined by the FTIR spectra and shown in Fig. 6. As the CH_4/SiH_4 flow ratio was varied from 0.5 to 10, the carrier gas flow rate remained constant at 100 sccm. In Fig. 6a (Ar is the carrier gas), we can clearly observe that when the CH_4/SiH_4 flow ratio is 0.5, the spectrum only exhibits the peaks of Si and SiO$_2$. When the CH_4/SiH_4 flow ratio is 1 or higher, the peak, which appears at 800 cm^{-1} indicate the formation of SiC. However, it was observed that SiC films could be deposited at a CH_4/SiH_4 flow ratio of 2 or higher when H_2 was the carrier gas (Fig. 6b).

The deposition at various CH_4/SiH_4 flow ratios was also studied by mixing 25 sccm Ar and 75 sccm H_2 as the carrier gas. The result shown in Fig. 7 is very interesting because the formation of SiC can be observed at a CH_4/SiH_4 flow ratio of 1.5, which is between 1 and 2 when Ar and H_2 are used as the carrier gas, respectively.

4. Discussion

In plasma-enhanced depositions of thin films, many reactions are involved both in plasma phase and on the
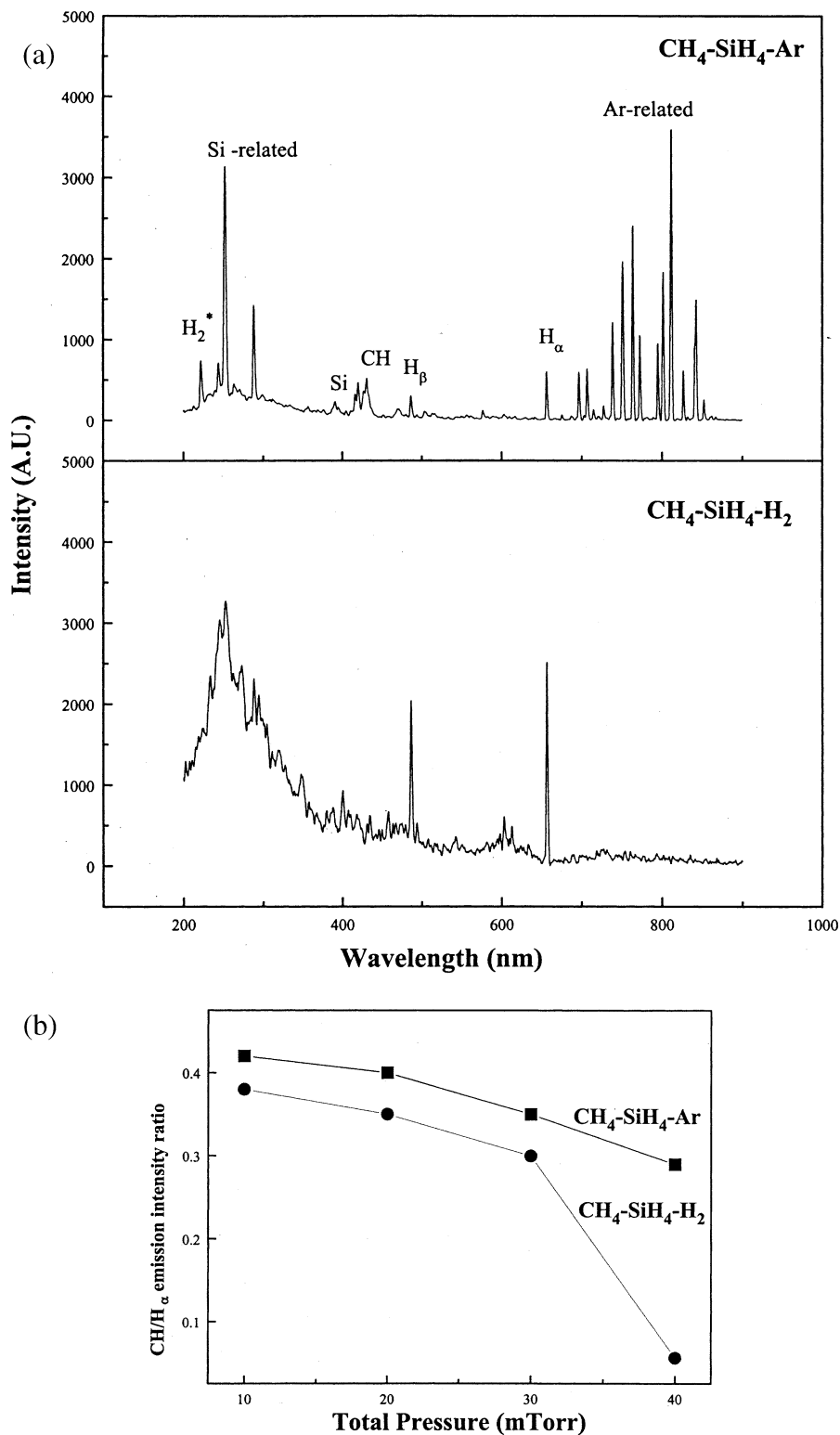
Fig. 2. (a) Typical in situ optical emission spectra of ECR plasmas for $CH_4/SiH_4/Ar$ and $CH_4/SiH_4/H_2$ gas systems, and (b) the CH (431 nm) to H_α emission intensity ratio as a function of total pressure.

substrate surface. Therefore, in order to obtain a desirable film composition and microstructure, it is important to understand the mechanism that governs the film formation. It is known that the dissociation of SiH_4 in a discharge essentially generates SiH_2 and SiH_3 radicals [17].
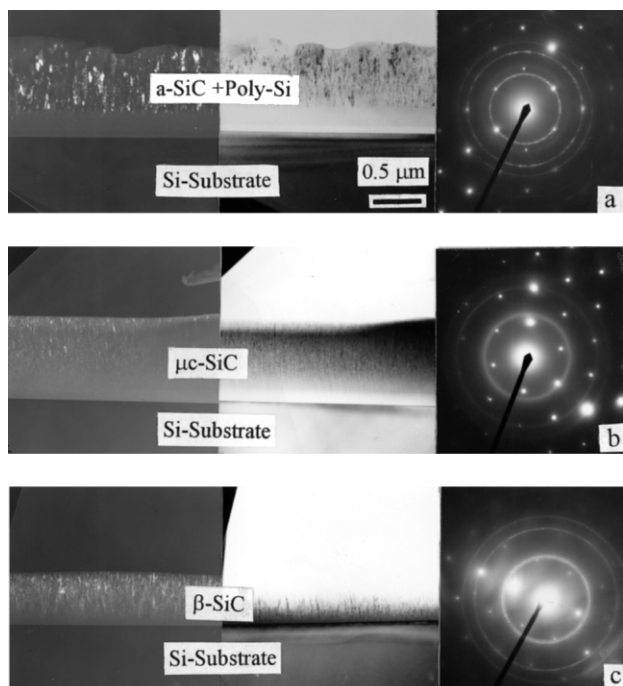
Fig. 3. XTEM dark-field and bright-field micrographs with diffraction patterns of the films deposited at 200°C, 1200 W, $CH_4/SiH_4/Ar = 5/2.5/100$, and a total pressure of (a) 40, (b) 30, and (c) 20 mtorr.
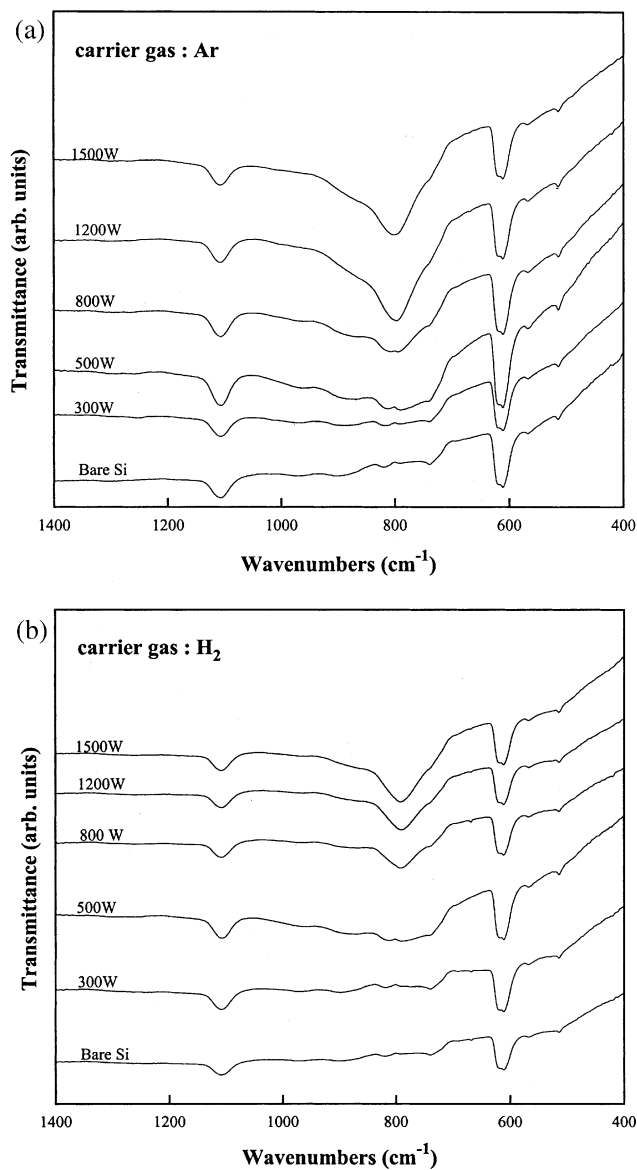
$$SiH_{4(g)} \rightarrow SiH_{x(g)} + \frac{4-x}{2}H_{2(g)} \qquad x = 2,3 \qquad (1)$$
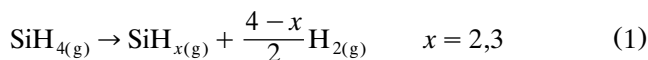
SiH_2 and SiH_3 radicals can decompose into Si by the following reaction [18,19].
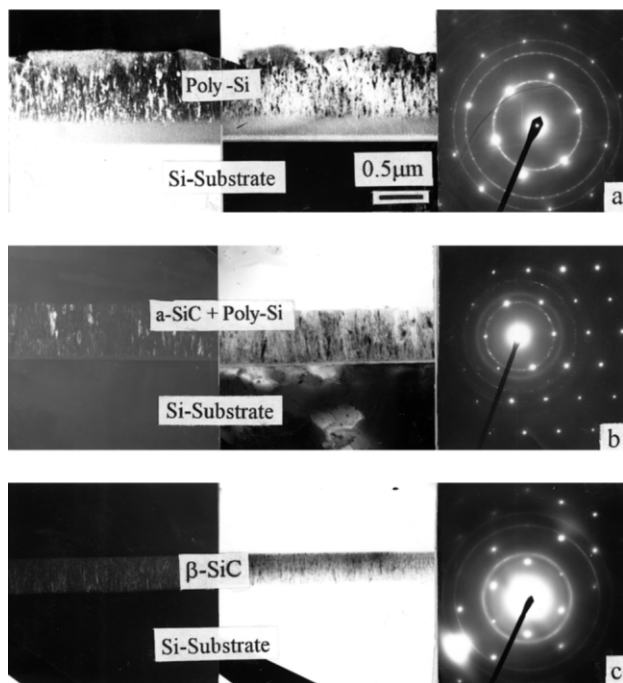
Fig. 4. XTEM dark-field and bright-field micrographs with diffraction patterns of the films deposited at 200°C, 1200 W, $CH_4/SiH_4/H_2 = 5/2.5/100$, and a total pressure of (a) 40, (b) 30, and (c) 20 mtorr.
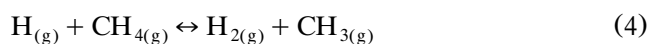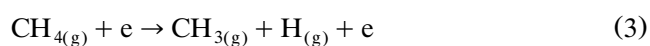

Fig. 5. FTIR transmission spectra of the Si substrate and the films deposited at 200°C, 20 mtorr, $CH_4/SiH_4 = 2$, various microwave powers, with (a) Ar as the carrier gas, and (b) H_2 as the carrier gas.

$$SiH_{x(g)} \rightarrow Si_{(s)} + \frac{x}{2}H_{2(g)} \qquad x = 2,3 \qquad (2)$$
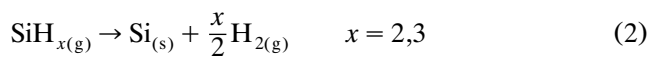
In plasma, methyl can be formed by the direct dissociation of methane. Also, methane can react with the hydrogen atom to form methyl [20].

$$CH_{4(g)} + e \rightarrow CH_{3(g)} + H_{(g)} + e \qquad (3)$$

$$H_{(g)} + CH_{4(g)} \leftrightarrow H_{2(g)} + CH_{3(g)} \qquad (4)$$

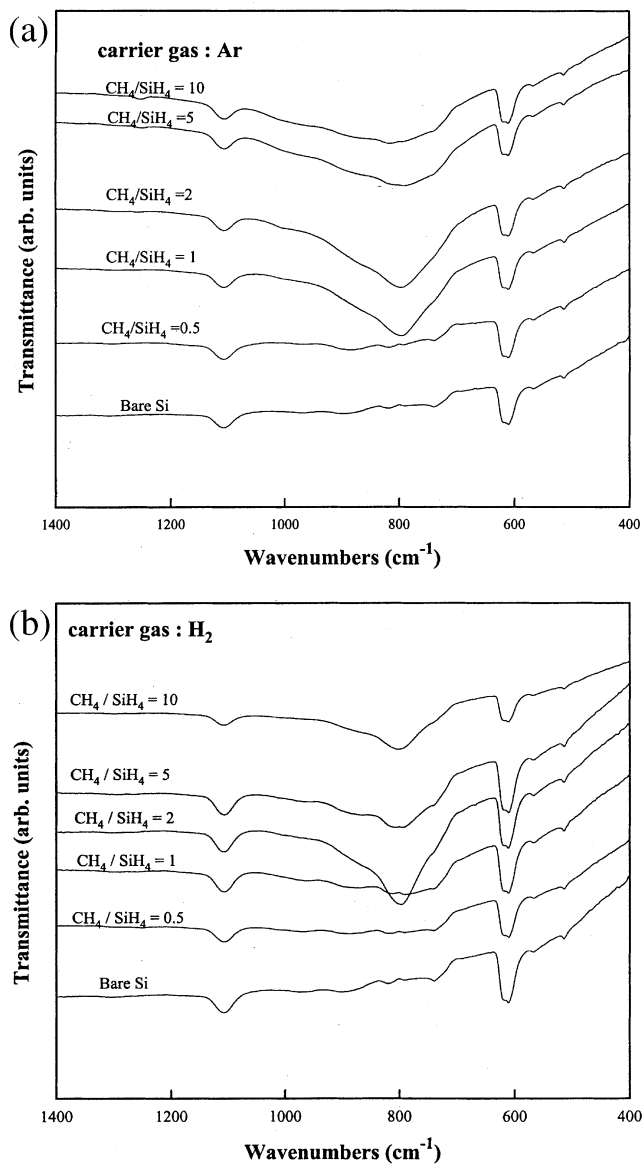Under the condition of excess hydrogen as in this study, the acetylene can be formed by the neutral–neu-

Fig. 6. FTIR transmission spectra of the Si substrate and the films deposited at 200°C, 1200 W, 20 mtorr, various CH_4/SiH_4 flow ratios, with (a) Ar as the carrier gas, and (b) H_2 as the carrier gas.

tral reaction of two methyl groups. This reaction can form C_2H_6 then, result in C_2H_2 following a series of H abstraction reactions [20].
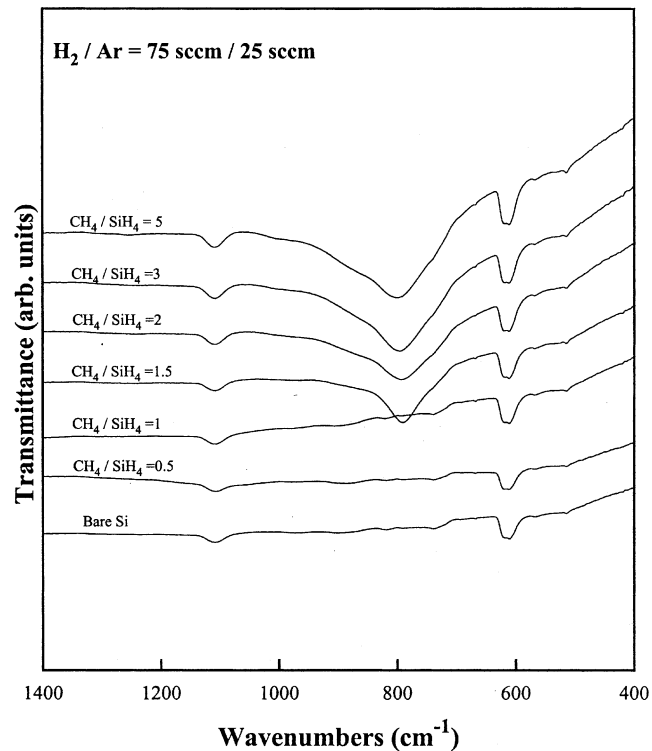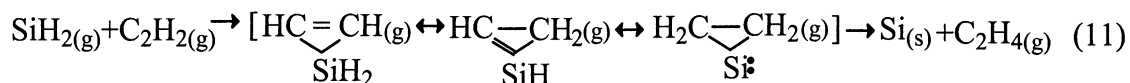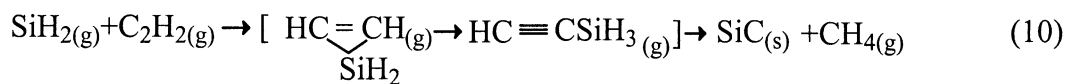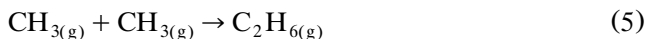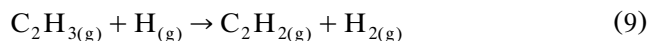
$$CH_{3(g)} + CH_{3(g)} \rightarrow C_2H_{6(g)} \tag{5}$$
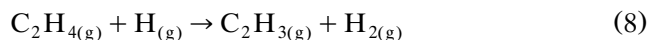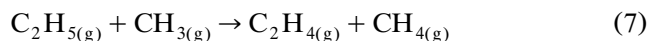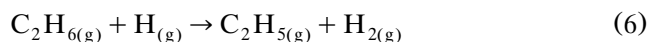

Fig. 7. FTIR transmission spectra of the Si substrate and the films deposited at 200°C, 20 mtorr, 1200 W, $H_2/Ar = 75/25$, and various CH_4/SiH_4 flow ratios.

$$C_2H_{6(g)} + H_{(g)} \rightarrow C_2H_{5(g)} + H_{2(g)} \tag{6}$$

$$C_2H_{5(g)} + CH_{3(g)} \rightarrow C_2H_{4(g)} + CH_{4(g)} \tag{7}$$

$$C_2H_{4(g)} + H_{(g)} \rightarrow C_2H_{3(g)} + H_{2(g)} \tag{8}$$

$$C_2H_{3(g)} + H_{(g)} \rightarrow C_2H_{2(g)} + H_{2(g)} \tag{9}$$

SiH_2 may react with C_2H_2 in two paths: (i) a gas-phase reaction between gaseous SiH_2 and gaseous C_2H_2 to form an intermediate product, probably $SiH_3C\equiv CH$ or $\overset{H_2C-CH_2}{\underset{Si:}{\vee}}$ then, adsorbing and decomposing into SiC or Si, respectively, on the surface as proposed by Erwin et al. [21], and (ii) a reaction of the

$$SiH_{2(g)} + C_2H_{2(g)} \rightarrow [\;HC\underset{SiH_2}{=}CH_{(g)} \rightarrow HC\equiv CSiH_{3\,(g)}] \rightarrow SiC_{(s)} + CH_{4(g)} \tag{10}$$

$$SiH_{2(g)} + C_2H_{2(g)} \rightarrow [HC\underset{SiH_2}{=}CH_{(g)} \leftrightarrow HC\underset{SiH}{-}CH_{2(g)} \leftrightarrow H_2C\underset{Si:}{-}CH_{2(g)}] \rightarrow Si_{(s)} + C_2H_{4(g)} \tag{11}$$
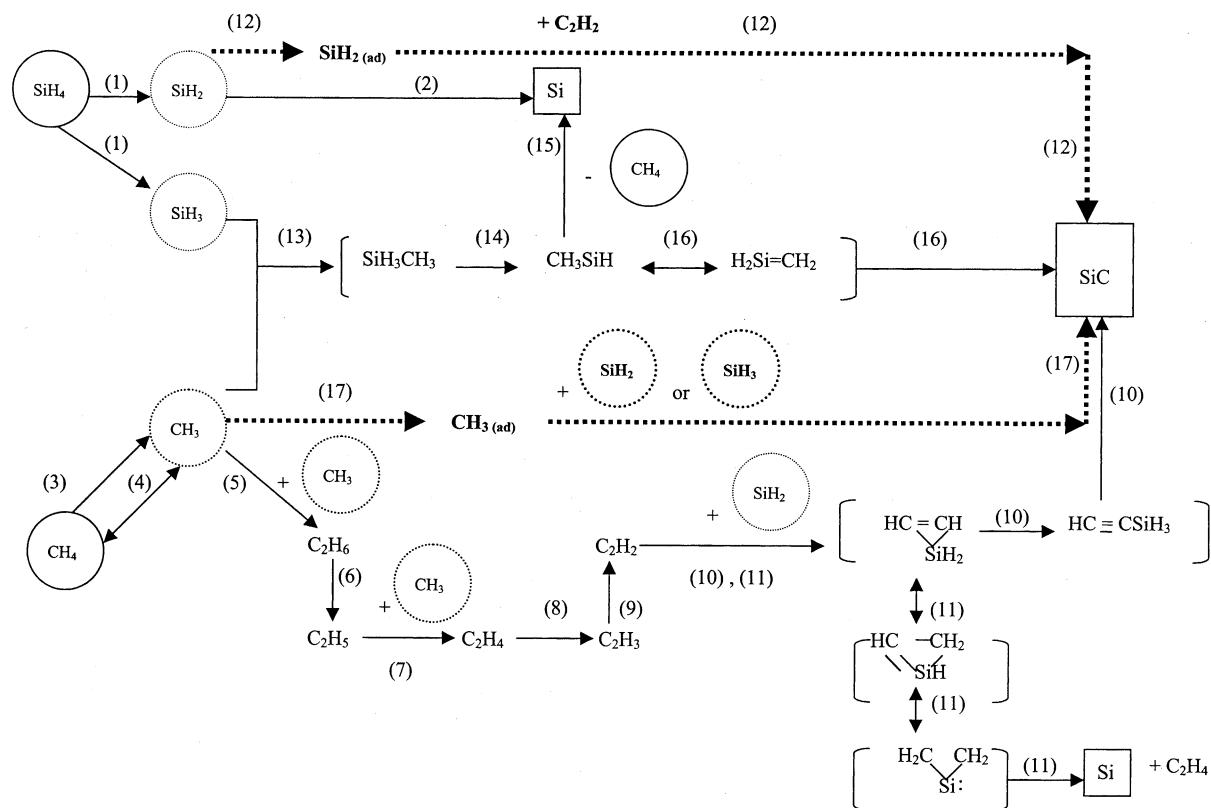
Fig. 8. Proposed growth mechanism for SiC thin films with SiH_4 and CH_4 as the source gases.

gaseous C_2H_2 with SiH_2 adsorbed on the surface to form SiC.

$$2SiH_{2(ad)} + C_2H_{2(g)} \rightarrow 2SiC_{(s)} + 3H_{2(g)} \qquad (12)$$
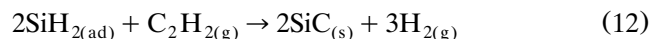
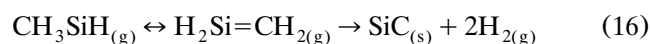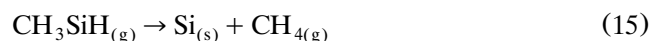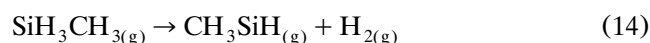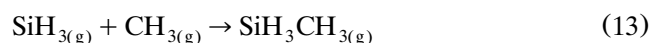On the other hand, SiH_x may react with CH_y in two paths: (i) a gas-phase reaction between gaseous SiH_3 and gaseous CH_3 to form an intermediate product [22], most probably CH_3SiH or $H_2Si=CH_2$ resulting in Si or SiC, respectively, as proposed by Johnson et al. [23,24],

$$SiH_{3(g)} + CH_{3(g)} \rightarrow SiH_3CH_{3(g)} \qquad (13)$$

$$SiH_3CH_{3(g)} \rightarrow CH_3SiH_{(g)} + H_{2(g)} \qquad (14)$$

$$CH_3SiH_{(g)} \rightarrow Si_{(s)} + CH_{4(g)} \qquad (15)$$

$$CH_3SiH_{(g)} \leftrightarrow H_2Si=CH_{2(g)} \rightarrow SiC_{(s)} + 2H_{2(g)} \qquad (16)$$

and (ii) a reaction of the gaseous SiH_x with CH_3 adsorbed on the surface to give SiC

$$SiH_{x(g)} + CH_{3(ad)} \rightarrow SiC_{(s)} + \frac{3+x}{2}H_{2(g)} \qquad (17)$$
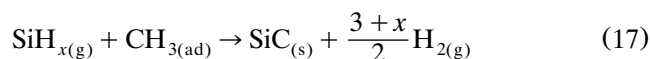
The dotted arrows indicate the reaction between the adsorbed and gaseous species. Based on the above discussion, the most probable film formation mechanism for the present work is summarized in Fig. 8.

The bond energies of Si–H and C–H are 70.4 and 98.8 kcal/mol [25], respectively. If the effective discharge powers for dissociation are equal, the dissociation of CH_4 is more difficult than that of SiH_4. From the results of OES (Fig. 2), it is clear that the CH/H_α emission intensity ratio decreases with the increasing gas pressure. This indicates that at higher total pressure the generation of atomic hydrogen is promoted and the formation of CH_3 radicals is inhibited. However, total pressure has a less effect on the decrease of CH/H_α emission intensity ratio, which represents the concentration of CH_3 when Ar is the carrier gas.

As shown in Fig. 1b and Fig. 4, when H_2 is the carrier gas, the deposited films become poly-Si as the total pressure is increased to 40 mtorr. This is because the generation of CH_3 radicals is inhibited at higher pressure as mentioned earlier, as a result less amount of CH_3 radicals impinging onto the substrate surface. Reactions (1) and then (2) become the dominant route for the deposition of poly-Si. However, when Ar is the carrier gas, we can clearly observe (Fig. 1a) that all spectra except bare Si substrate exhibit the main peak at 800 cm^{-1} of the Si–C bond at all pressures. This

also indicates that total pressure has a less effect on the concentration of CH_3 when Ar is the carrier gas. The results of TEM (Fig. 3) show that a film of poly-Si grains embedded in a-SiC was deposited at a higher pressure (40 mtorr), whereas β–SiC was formed at a lower pressure (20 mtorr and below). This also indicates that the number of CH_3 radicals reaching the growing surface is smaller at high pressure. Therefore, FTIR and TEM results are consistent with those of OES due to the same reasons.

Based on the above discussion, the formation of various type films at different CH_4/SiH_4 flow ratios and microwave powers can also be explained as follows. From the results shown in Fig. 6b, in the case of CH_4/SiH_4 flow ratios below 2 when H_2 is the carrier gas, most of the SiH_4 decomposes into SiH_3, SiH_2 and silicon. However, only a small quantity of CH_4 decomposes into CH_3. The decomposition reaction of SiH_4 [Eq. (1)] should dominate and result in large amount of SiH_x radicals. The SiH_x radicals adsorb onto the Si surface where they decompose and polycrystalline silicon is deposited [Eq. (2)]. At a CH_4/SiH_4 flow ratio of 2, relatively larger amounts of the CH_4 is added into the system. The amounts of CH_3 radicals and C_2H_2 are comparable with that of SiH_x, so that Eqs. (10), (12), (16) and (17) of the mechanism could occur to form SiC. However, the SiC films could be deposited at 1 and higher CH_4/SiH_4 flow ratios when Ar is the carrier gas (Fig. 6a). This is because CH_4 is more effectively decomposed in ECR plasma when Ar is the carrier gas and the heavy mass of Ar produces significant increase in the momentum of radicals and cause Eqs. (10), (12), (16) and (17) to occur at $CH_4/SiH_4 = 1$. For the same reason, the formation of SiC using a mixture of 25% Ar in H_2 as the carrier gas at a CH_4/SiH_4 flow ratio of 1.5 (Fig. 7) is obvious.

When the microwave power is as low as 300 W, the deposited film is still poly-Si (Fig. 5) even at a CH_4/SiH_4 flow ratio of 2. That is because the energy needed for SiH_x formation is lower than that of CH_3 and the energy is enough for the subsequent decomposition of SiH_x to occur. However, at 500 W and above the energy supplied by plasma may be enough for the dissociation of CH_4 so that most SiH_x radicals can react with CH_3 radicals and C_2H_2 to form SiC. This is because CH_4 has a lower dissociation efficiency than SiH_4. The results obtained at different flow ratios and microwave powers indicate that the dissociation of CH_4 should be the rate-limiting step.

5. Conclusion

ECR-CVD has been employed to prepare β–SiC films using $CH_4/SiH_4/H_2$ or $CH_4/SiH_4/Ar$ mixtures. The deposited films were characterized with XTEM, OES, and FTIR. The results indicate that the carrier gases have a greater influence on the film composition and microstructure as compared to the growth parameters like pressure, power and flow ratio. Based on the proposed film formation mechanism in combination with experimental results, we found that the dissociation of CH_4 is the rate-limiting step for the growth of SiC irrespective of whether Ar or H_2 as the carrier gas. At higher total pressure, the generation of atomic hydrogen is promoted and the formation of CH_3 radicals is inhibited. In contrast to H_2, total pressure has less effect on the concentration of CH_3 when Ar is the carrier gas. Ar is more effective in the dissociation of reactant gases than H_2.

References

[1] M. Bhatnagar, B.J. Baliga, IEEE Trans. Electron Dev. 40 (1993) 645.
[2] J.D. Hwang, Y.K. Fang, Y.J. Song, D.N. Yaung, Jpn. J. Appl. Phys. 34 (1995) 1447.
[3] H.J. Kim, R.F. Davis, J. Appl. Phys. 60 (1986) 2897.
[4] E.G. Wang, Physica B 185 (1993) 85.
[5] T. Takeuchi, H. Amano, K. Hiramatsu, N. Sawaki, I. Akasaki, J. Cryst. Growth 115 (1991) 634.
[6] M. Diani, J.L. Bischoff, L. Kubler, D. Bolmont, Appl. Surf. Sci. 68 (1993) 575.
[7] M. Katsuno, T. Futagi, Y. Ohta, H. Mimura, K. Kitamura, Appl. Surf. Sci. 70/71 (1993) 675.
[8] K.L. Cheng, H.C. Cheng, C.C. Liu, C. Lee, T.R. Yew, Jpn. J. Appl. Phys. 34 (1995) 5527.
[9] T. Futagi, M. Katsuno, N. Ohtani, H. Mimura, K. Kawamura, Appl. Phys. Lett. 58 (1991) 2948.
[10] C.H. Chen, C.M. Wan, T.R. Yew, Appl. Phys. Lett. 62 (1993) 3126.
[11] P.J. Grunthaner, F.J. Grunthaner, R.W. Fathauer et al., Thin Solid Films 183 (1989) 197.
[12] Y. Sun, T. Miyasato, J.K. Wigmore, J. Appl. Phys. 85 (1999) 3377.
[13] A. Chayahara, A. Masuda, T. Imura, Y. Osaka, Jpn. J. Appl. Phys. 25 (1986) L564.
[14] P. Rai-Choudhury, N.P. Formigoni, J. Electrochem. Soc. 116 (1969) 1440.
[15] D.S. Kim, Y.H. Lee, J. Electrochem. Soc. 142 (1995) 3493.
[16] C.C. Liu, C. Lee, K.L. Cheng, H.C. Cheng, T.R. Yew, Appl. Phys. Lett. 66 (1995) 168.
[17] M.D. Shieh, C. Lee, C.H. Cheng, T.R. Yew, C.Y. Kung, Appl. Phys. Lett. 63 (1993) 1252.
[18] J.H. Lee, S.K. Park, C.S. Kim, Jpn. J. Appl. Phys. 34 (1995) L1191.
[19] M. Zhang, Y. Nakayama, S. Nonoyama, K. Wakita, J. Non-Cryst. Solids 164 & 166 (1993) 63.

[20] W.L. Hsu, J. Appl. Phys. 72 (1992) 3102.

[21] J.W. Erwin, M.A. Ring, H.E. O'Neal, Int. J. Chem. Kinet. 17 (1985) 1067.

[22] Y. Catherine, G. Turban, B. Grolleau, Thin Solid Films 76 (1981) 23.

[23] A.D. Johnson, J. Perrin, J.A. Mucha, D.E. Ibbotson, Mater. Res. Soc. Symp. Proc. 282 (1993) 451.

[24] A.D. Johnson, J. Perrin, J.A. Mucha, D.E. Ibbotson, J. Phys. Chem. 97 (1993) 12937.

[25] J. Saraie, Thin Solid Films 117 (1984) 59.